X-Ray Computed Tomography versus Metallography for Porosity Analysis in Aluminium RPT Castings

J.L. Malisano, S. Kumar, C.M.A Lui, and K.A.Q O'Reilly
Department of Materials, *University of Oxford, Parks Road, Oxford, OX1 3PH, United Kingdom*

Abstract

X-Ray Computed Tomography (XCT) is compared with metallography for the evaluation of the size, morphology, and distribution of pores in Al-Si Reduced Pressure Test castings (RPTs) in 3D and 2D, respectively. The results showed that porosity assessment in 3D was more effective than in 2D, due to the highly connected pore structure that forms in RPTs which cannot be adequately represented by the latter technique. The uncertainty in the 3D measurements that is introduced by sub-voxel pore features was shown to have a significant impact on the accuracy of the analysis, but even so it compared better to that determined by the Archimedes' principle than the 2D technique for evaluating the fraction of porosity in the samples.

Keywords: X-Ray Tomography, Cast Aluminium, Porosity

1. Introduction

Porosity is one of the major defects that forms from dissolved hydrogen and volumetric shrinkage of the metal during solidification in Al alloys [1, 2]. The conventional approach to evaluating the morphology and spatial distribution of porosity in castings is by metallographic analysis over a cross-sectional plane. Not only is this intrinsically destructive, but the measured properties are confined to two dimensions (2D) on the analysis plane. Hence the third dimension of information is lost. Moreover, extrapolation of 2D measurements of porosity into three dimensions (3D), when pore geometries can be complex and inhomogeneous, may be misleading or erroneous [3].

X-Ray Computed Tomography (XCT) offers a non-destructive approach for quantitatively measuring porosity in cast materials – particularly Al and other light metals due to X-Ray transmissibility – in 3D and 4D (3Dtime-lapse) [4, 5]. XCT for the assessment of porosity is becoming increasingly popular in Materials Science, with the number of publications increasing significantly between the year 2000 and February 2017 as shown in Figure 1. One of the main limitations of XCT is the resolution of X-ray detectors, which have limited the physical size of the samples that can be analysed at high resolution, as there is a trade-off between scan area and resolution [5]. As such, quantitative micro-analysis with laboratory XCT systems has generally been restricted to samples ~10mm in size, or regions of interest in in samples 20mm diameter [4]. In studies of cast Al there have been a few studies that have evaluated porosity in Reduced Pressure Test castings (RPT) [6, 7] – 40mm in diameter at their thickest -, a staple test of melt quality in the casthouse. Conventionally, the size and

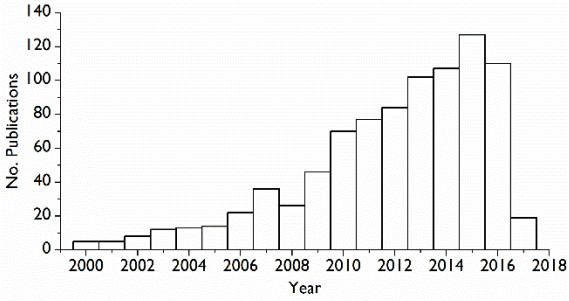

Figure 1: The number of publications returned by a search of Scopus [8] on porosity analysis with X-Ray Tomography in February 2017.

structure of porosity in RPTs is evaluated in 2D by metallography. However, there has yet to be a systematic study that compares the results of a 3D analysis of porosity in RPTs using XCT, which can properly account for the extensive interconnectivity of pores in these castings, to the conventional 2D analysis of a cross-section area with metallography.

In this work XCT and metallography are used to assess the number, fraction, morphology, and spatial distribution of porosity throughout the entirety of Al-Si alloy RPTs. The results of each technique will then be compared, and their efficacy for porosity evaluation in RPTs discussed. In particular, the interconnectivity of pores on porosity measurements will be examined.

2. Experimental Method

2.1 Materials and Casting

Two charges of ~40kg of Al-3(wt.%)Si and Al-7Si were melted in a resistance heated furnace, held at 730°C, and upgassed by bubbling an Ar-15H gas mixture from the

bottom using a submerged lance. The purpose of up-gassing was to obtain reproducible high hydrogen levels, at constant hydrogen partial-pressure, in both alloys, which, from 2D analyses, has been reported to strongly influence the size, number, and morphology of pores in Al castings [1, 2]. A reduced pressure test (RPT) was cast from the melt and solidified at 80mBar pressure with 4 minutes of reduced pressure application. Table 1 shows the nominal composition and hydrogen content at the time of casting, measured using a Spectrolab LAVFA05A spark analyser optical emission spectrometer and an AlSCAN™ Model F (ABB).

Table 1: Composition and hydrogen level of the alloys

Alloy	Composition (wt.%) Si	Fe	Mg	Ti	Hydrogen (ml 100g^{-1})
Al-3%Si	3.022	0.180	0.009	0.005	0.435
Al-7%Si	6.970	0.020	0.010	0.006	0.393

2.2 Porosity Characterisation

The density of the RPTs was measured in water using Archimedes' principle, from which the "Archimedes'" volume of porosity inside was calculated using the theoretical alloy densities. The theoretical densities were calculated to be 2.698 and 2.683 g cm^{-3} for the Al-3Si and Al-7Si alloys, respectively, using the rule of mixtures and a 1.2wt.% solubility of Si in Al [9].

The porosity in the RPTs was subsequently assessed in 3D using XCT. A North Star Imaging ImigiX system was used to scan the entire RPTs with a nominal resolution (voxel size) of approximately 49µm – although it is difficult to accurately define the resolution of XCT systems due to the interplay of a number of factors as discussed by others [4, 5, 10]. The XCT data were then analysed with Avizo 9.2 software (FEI, USA). A non-local means filter [11] was applied to the data, and a match contrast function was applied to normalise the grayscale intensities of the Al-7Si data to the Al-3Si data. Strong pores were then segmented using the Otsu method [12], while weaker pores were segmented using a black Top-Hat algorithm with a small kernel size and the gradient threshold set to approximately twice that of the noise gradient in the metal. The number, volume, equivalent spherical diameter (Equation 1), spatial distribution, and sphericity (Equation 2) of the pores was then characterised along with the metal volume.

$$D_s = \left(\frac{6}{\pi}V\right)^{\frac{1}{3}} \quad (1)$$

$$\psi_s = \frac{(\pi\,(6V)^2)^{\frac{1}{3}}}{A} \quad (2)$$

Where V and A are the pore volume and surface area, respectively. Pores with a volume ‹8 voxels were excluded from the analysis altogether, and only pores › 125 voxels were used for morphological analysis [13]. The uncertainty in this analysis was taken to be ± 1 voxel either side the pore surface voxels (voxels without at least 1 nearest neighbour), due to difficulty in defining the border between pore and metal at sub-voxel resolution and the uncertainty of volume and interconnectivity of each phase within these voxels. A qualitative 2D representation of this concept is show in Figure 2, with the voxel intensities, and segmentation not accurately defining the size or morphology of the pore's sub voxel features – indeed the single pore is represented as two individual pores.

Following the XCT scans, metallography was conducted on the RPTs to assess the porosity. The RPTs were sectioned longitudinally down their centre, the cross-sectioned faces of both halves of the sample were then sprayed with matte black paint – to increase pore contrast with the metal substrate – and ground to a 9µm surface finish. The two halves of each of the samples were then scanned at 3200dpi (7.9 µm per pixel) using an Epson 3490 Photo office scanner. 2D analysis of the scanned RPT surfaces was then performed with Fiji [14]. A bilateral filter with a large kernel size was applied to the image before the pores were segmented using the Otsu method – again restricting the threshold calculation to inside the RPT. The Fiji 'Particle Analyser' plugin was then used to measure the number, area, equivalent circular diameter (Equation 3), spatial distribution, and circularity (Equation 4) of the pores, along with the metal area.

$$D_s = 2\sqrt{\frac{A}{\pi}} \quad (3)$$

$$\psi_s = \frac{4\pi A}{P^2} \quad (4)$$

Where A and P are the pore area and perimeter, respectively. Pores ‹ 4 pixels were excluded from the analysis all together, and only pores › 25 pixels were used for morphological analysis. The uncertainty for this analysis was taken to be the measurement variation between the two halves of the RPT as it is more significant than measurement errors.

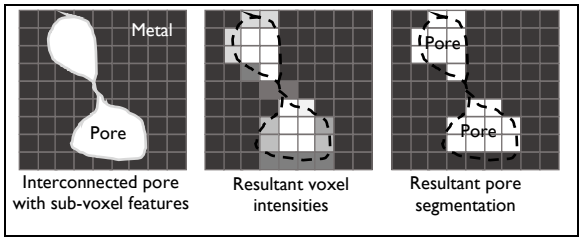

Figure 2: The effect of sub-voxel pores / pore features on the resultant voxel intensities in the image, and the resultant pore segmentation.

3. Results and Discussion

Figure 3 shows the measured pore fraction by XCT in 3D and Metallography in 2D compared against that calculated by the conventional approach for evaluating porosity volume fraction in RPTs, the Archimedes' principle. It shows that there is a reasonable agreement between the Archimedes' porosity and that measured by XCT analysis, although there is a considerable spread due to uncertainty in the XCT measurement. This is introduced by surface voxels of the pores, the addition or subtraction of which results in a considerable increase or decrease in pore volume – particularly in small and interdendritic pores, which have

a high surface area to volume ratio and are therefore more sensitive to this uncertainty. Comparatively, there is a significant difference between the Archimedes' porosity and that measured by the metallographic analysis, although there is less variation due to measurement uncertainty than in the 3D analysis. Even with the maximum uncertainty, the 3D analysis gives a closer result to the Archimedes' pore volume. This demonstrates that a 2D analysis of pore area fraction is not representative of the pore volume fraction, which is in agreement with the findings of Anyalebechi [1]. Whereas a 3D analysis, with the correct parameters and adequate resolution, is more representative of the pore volume fraction in the sample. This is especially true for alloys that develop a network of shrinkage pores around their centre – such as the Al-7Si alloy for example.

Also shown in Figure 3 is a comparison of the pore number density in the RPTs measured by XCT and metallography, and shows a considerable discrepancy between the two techniques. XCT measures a lower pore number density (pores per unit volume) in both of the alloys, especially in the Al-7Si sample compared to metallography (pores per unit area). In the Al-3Si alloy, this is likely due to the inadequacy of 2D analysis for accurately representing porosity over the entirety of the sample. In the Al-7Si, this is due to the extensive interconnected shrinkage porosity, which, when viewed from a 2D plane, appears as a dense collection of small individual pores, although it is a single, tortuous, interconnected structure in 3D. An example of this is shown in Figure 4, which compares the number of individual pores – labelled with distinct colours – in 3D (a) and 2D (b) analysis. Many pores are labelled as individual in the 2D analysis, though in 3D they are interconnected. The true scale of 3D pore interconnectivity is also shown on the same plane of 2D analysis in Figure 4 c). Finally, it should be noted that the considerable variation in the XCT pore number density measurement arises due to uncertainty from surface voxels on the connectivity of pores – which can connect or disconnect individual pores, making them seem less or more numerous.

From herein, only results for the Al-7Si alloy will be presented for the purpose of brevity, though those of the Al-3Si sample will still be discussed.

Figure 5 shows a comparison of the spatial and volume distributions of individual pores (the distance of their centroid from the *z*-centroid of the RPT) in the Al-7Si alloy RPT. 3D analysis of the pore distributions counts a greater number of individual pores (though the pore number density is lower) compared to the 2D analysis; this is also observed in the Al-3Si alloy RPT. The frequency distribution of pore position is also more thoroughly represented in the 3D analysis compared to the 2D analysis. 3D results show a normal frequency distribution, while the 2D analysis takes the shape of a plateau distribution, with a right hand skew – though it has a shape reminiscent of the 3D results. In the Al-3Si alloy the pores show a bimodal frequency distribution, with a slight left skew, whereas the metallography shows a plateau frequency distribution. The spatial distribution of pores measured by the 3D analysis porosity volume throughout the across the casting also varies strongly between the analysis methods. 3D analysis shows that a vast majority of the pore volume is concentrated in a single location – the centroid of the large pore network, the one which is shown in Figure 3 b) and c) –whereas it is distributed more homogenously in the 2D analysis. Again, this is the same trend as what is measured in the Al-3Si alloy. The effect of measurement uncertainties in the 3D analysis is not shown here, but they have the effect of linking up or delinking the extensive pore networks, thus increasing or decreasing the overall pore count and increasing or decreasing the fraction of pore volume locked up in these networks. Finally, also of note, is the discrepancy between the overall spatial distribution range of the porosity. This is due to differences in the calculated moment of area from the radial-axis of the metallographic plane and 3D reconstruction.

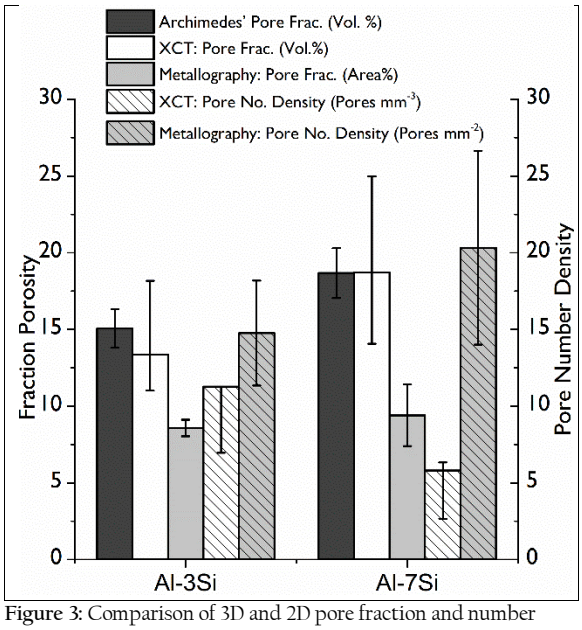

Figure 3: Comparison of 3D and 2D pore fraction and number density by XCT and metallography, respectively.

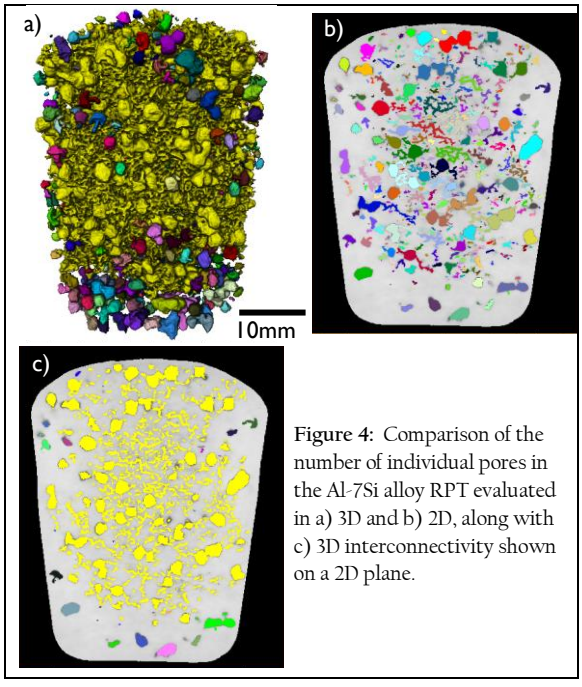

Figure 4: Comparison of the number of individual pores in the Al-7Si alloy RPT evaluated in a) 3D and b) 2D, along with c) 3D interconnectivity shown on a 2D plane.

The distribution of Figure 6 shows the size and shape distribution of pores as measured by 2D and 3D analysis in the Al-7Si alloy. The sphericity and circularity are a measure of how spherical or circular the pores are, with a value of 1 representing a circular pore, such as a gas pore, and decreasing values representing increasingly irregularly shaped pores, such as interdendritic pores. The graphs show that there is a very strong right skew to smaller pore sizes, in both analyses, with a similar distribution of pore sizes. Smaller pore sizes are resolved in the 2D analysis than in 3D, due to resolution limits of the XCT equipment, though the 3D analysis detects more pores overall. The 2D analysis is able to resolve smaller pores than the 3D analysis, however the true size and inter-connectivity of pores is only represented by the 3D analysis, which shows the presence of a single, large, non-spherical (<0.25) pore – the inter-connected pore network that is visible in Figure 4 a). The 3D analysis shows a higher incidence of round pores (sphericity >0.75) than the 2D analysis, where most pores are irregularly shaped (circularity <0.5) - this arises from the 2D representation of interdendritic pores. Similar results are observed in the Al-3Si Alloy RPT, though the large interconnected pore network has a smaller equivalent spherical diameter – indicating that it is not as extensive as that in the Al-7Si RPT. Finally, again the measurement uncertainties in the 3D analysis are not shown, but they have the effect of linking up or delinking the extensive pore networks, thus increasing or decreasing the overall pore count and increasing or decreasing the sphericity of these networks.

4. Summary & Conclusions

XCT has been used to assess the porosity throughout RPT castings solidified at 80mBar reduced pressure in 3D, and the results compared to a conventional 2D analysis by metallography. While there is considerable uncertainty in the 3D XCT measurements due to the effect of sub-voxel pore features and lower resolution compared to the 2D analysis, the results show that it can be used to more effectively characterise volume fraction, number density spatial distribution, and morphology of porosity in RPTs. This is due to the very extensive pore connectivity that develops in these types of castings, which is not adequately represented in 2D; especially, but not exclusively in alloys that develop interdendritic shrinkage porosity. The segmentation parameters of the 3D analysis requires careful selection so as to not over- or under-segment porosity as it can significantly alter the results, as is indicated by the uncertainty in the measurements. However, even with the maximum uncertainty, the 3D measurements of pore fraction showed closer agreement than the 2D analysis with the pore fraction calculated from Archimedes' method. Increased XCT resolution can significantly reduce the uncertainty in 3D porosity analysis.

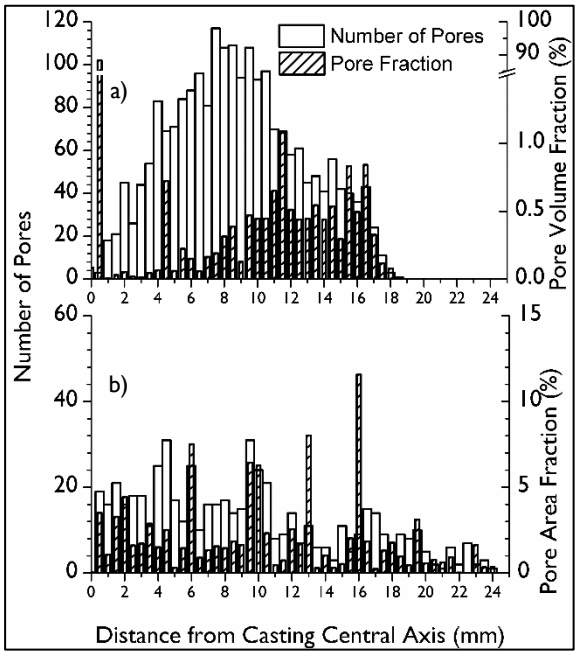

Figure 5: Spatial distribution of pores from the central axis in the RPT measured in a) 3D and in b) 2D in the Al-7Si alloy.

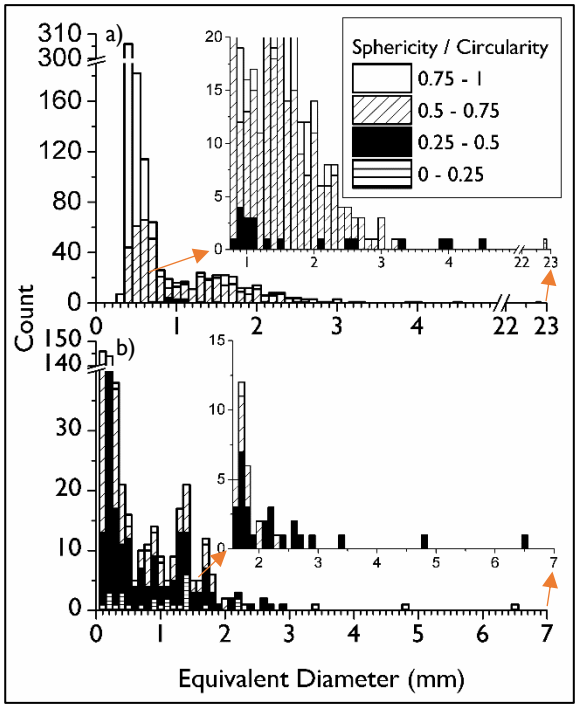

Figure 6: Pore size and shape distribution of pores in the Al-7Si alloy from a) 3D and b) 2D analyses.

Acknowledgements

The authors are grateful to Dr. Enzo Liotti for his assistance with the data analysis, and acknowledge EPSRC grants (EP/J013501/1) and (EP/M02833X/1) for the University of Oxford Experimental Equipment Upgrade.

References

1. P. Anyalebechi, *J. Mat. Sci*, 2013, **48**: 5342.
2. R.C. Atwood *et al.*, *Acta Mater.*, 2008, **48**: 405.
3. G. Nicoletto *et al.*, *Procedia Eng.*, 2010, **2**: 547.
4. S.R. Stock, *Int. Mater. Rev.*, 2008, **53**: 129.
5. E. Maire, P.J, Withers, *Int. Mater. Rev.*, 2014, **59**: 1.
6. D. Eskin *et al.*, *Mat Sci Tech Ser,*, 2015, **31**: 79.
7. T. Pabel *et al.*, *TMS Supp. Proc.: Gen. Paper Select.*, U.S.A, 2011, p.803.
8. Elsevier B.V., *Scopus [Electronic Database]*, 2017, Available from: https://www.scopus.com.
9. L.F. Mondolfo, *Al. Alloys: Struc. Prop.*, 1976, UK, p. 368.
10. J.P. Kruth *et al.*, *CIRP Ann-Manuf. Tech*, 2011, **60**: 821.
11. A.B. Buades *et al.*, IEEE CVPR *Conf. Proc.* 2005, p.60.
12. N. Otsu, *IEEE Trans. Syst.,Man. Cybern. Syst.*, 1975, **9**: 23.
13. F.S. Leonard *et al.*, Proc. 6th Conf. Indust. Comp. Tomo., 2016, p.1.
14. J., Schindelin *et at.*, *Nature Methods*, 2012, **9**: 676.